World Conference on Timber Engineering Oslo 2023

NUMERICAL AND EXPERIMENTAL STUDY OF GLULAM BEAMS JOINTED WITH SLOTTED-IN STEEL PLATE CONNECTION

Sigurdur Ormarsson[1], Le Kuai[2], Musaab Ahmed Mahjoub[3], Simon Aicher[4]

ABSTRACT: The present work focuses on analysis of deformation and strength behaviour of slotted-in steel plate connections in glued laminated timber (GLT). In Eurocode 5 (EC5), the design of metal dowel-type timber joints is based on the yield theory presented by Johansen [1]. It consists of analytical expressions to calculate the lateral load-carrying capacity of single fastener joints that exhibit different (plastic) failure modes. When designing optimised multiple fastener connections that are exposed to dominating moment action, the calculation of fastener forces and their directions during progressive plasticization of the dowel group is difficult to perform manually. Therefore, a simple numerical model to simulate progressive elasto-plastic force development for every individual dowel is needed. This study presents new and simple models to analyse the bending deformations of glulam beams jointed with mechanical slotted-in steel plate connections. The proposed models were experimentally verified using results obtained from a joint project with the Material Testing Institute (MPA) at University of Stuttgart.

KEYWORDS: Jointed timber beams, steel-to-timber joints, failure modes, FE-modelling, experiments

1 INTRODUCTION

This investigation arises from the increased usage of large timber trusses jointed with slotted-in steel plate connections in bridges, long-span roofs, and high-rise buildings. For these types of structures, deformation and strength behaviour of the connections are often critical elements in the design, especially if exposed to significant in-plane moment action during varying environmental conditions. The load-carrying capacity calculations of single and double shear joints, according to EC5, are based on the Johansen theory in [1]. According to this theory the joints fail in several plastic failure modes depending on the thickness of the wood members. The shear load carrying capacity for these failure modes differs significantly in size, depending on various parameters such as wood thickness, embedding strengths, dowel diameter and yield moment of the dowel. The embedding strengths are also highly influenced by the angles between the fastener forces and fibre directions of the wood members. In design of multi-dowel connections exposed to significant moment action, a typical hand calculation of the fastener forces and their directions is too simple since the slip modulus does not consider the angle between the fastener force and the fibre direction. To study how fastener forces and their directions vary during progressive plasticization in different dowel groups, simple finite element models need to be developed. Some 3D numerical models to simulate the mechanical behaviour of multiple fastener connections have been published in recent decades, see e.g. [2–5]. These models allow for detailed analyses of the connections in terms of local slip deformations, dowel force distributions and timber failures. They are good for understanding and they can obtain results that are impossible to obtain from experiments. For example, they can show the difference in dowel force size and directions compared to the simple analytical approach used in EC5. As for disadvantage, these models are computationally costly and sometimes numerically unstable. However, the detailed results provided help us to limit the number of expensive experiments and develop more optimized and simpler analytical or numerical models. Some researchers have developed more efficient models to tackle the drawbacks of using 3D models. In [6], a two-dimensional finite element model was developed to simulate multi-dowel timber-to-timber moment-resisting connections. The timber was modelled as an elastic orthotropic material and each fastener was modelled with two nonlinear springs. A semi-analytical model based on kinematic compatibility and equilibrium considerations was presented in [7]. The disadvantage of this model is that it neglects the elastic timber deformations between the dowels. The beam on foundation modelling approach to calculate the slip displacements and load carrying capacity of the connection using nonlinear springs to simulate the embedment behaviour was also used in [8].

This study is based on the master thesis work presented in [9], where three simplified FE-models using structural elements were created to study the bending behaviour of jointed glulam beams using mechanical slotted-in steel plates. To verify the models, extensive experimental tests were performed at MPA, University of Stuttgart. The aim

[1] Sigurdur Ormarsson, Linnaeus University, Sweden, sigurdur.ormarsson@lnu.se
[2] Le Kuai, Linnaeus University, Sweden, le.kuai@lnu.se
[3] Musaab Ahmed Mahjoub, University of Navarra, Spain, mahmedmahjo@unav.es
[4] Simon Aicher, MPA University of Stuttgart, Germany, Simon.Aicher@mpa.uni-stuttgart.de

https://doi.org/10.52202/069179-0172

of this work was to develop effective and flexible engineering models useful when designing jointed glulam beams.

2 MODELLING

To study the slotted-in steel plate connection behaviour in the studied glulam beams, three different finite element models were created. The first was a parameterized single-dowel model for double shear joints; the second was a simple beam model to simulate the global bending deformations and (ideal plastic) load carrying capacity of glulam beams jointed with a slotted-in steel plate. The connection was modelled with two nonlinear connector elements for each dowel group. The final model was a combined beam-shell model of the same glulam member using a few connector elements to simulate each dowel in the dowel groups. This work focuses on developing simple and efficient models by using effective structural elements (beams, shells, and spring-based connector elements) to simulate both global bending deformations and local dowel force distributions in glulam members jointed with slotted-in steel plate connections.

2.1 MODELING OF SINGLE DOWEL JOINTS

For single dowel (slotted-in steel plate) joints loaded to failure, EC5 shows three (plastic) failure modes for different thickness ranges. In Figure 1, these failure modes together with curves (based on Eq. 1) illustrate how the shear load carrying capacity of the joint varies with increasing wood thickness. According to EC5 the shear load carrying capacity of the (slotted-in steel plate) joint is the minimum value obtained from the three following expressions in Eq. (1), where t is the thickness

$$\begin{bmatrix} F_{v,\alpha,Rk,I} \\ F_{v,\alpha,Rk,II} \\ F_{v,\alpha,Rk,III} \end{bmatrix} = \begin{bmatrix} f_{h,\alpha,k} t d \\ f_{h,\alpha,k} d \left[\sqrt{(t+2e)^2 + t^2 + \frac{4M_{y,Rk}}{f_{h,\alpha,k} d}} - (t+2e) \right] \\ f_{h,\alpha,k} d \left[\sqrt{e^2 + \frac{4M_{y,Rk}}{f_{h,\alpha,k} d}} - e \right] \end{bmatrix} \quad (1)$$

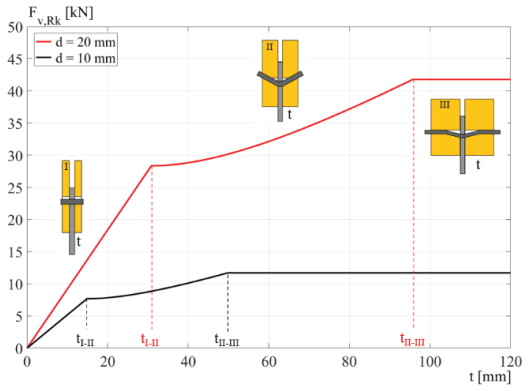

Figure 1: *Three failure modes for single dowel slotted-in steel plate joints together with two curves showing how the shear load carrying capacity varies with increasing wood thickness when* $\rho_k = 350\ [\frac{kg}{m^3}]$, $f_{u,k} = 400\ [MPa]$ *and* $\alpha = 0$.

of the wood members and d is the diameter of the dowel. The characteristic embedding strength of the wood material in the dowel force direction $f_{h,\alpha,k}$ and the characteristic yield moment of the steel fastener $M_{y,Rk}$ are given by

$$M_{y,Rk} = 0.3 f_{u,k} d^{2.6} \quad (2)$$

$$f_{h,\alpha,k} = \frac{0.082(1 - 0.01d)\rho_k}{k_{90} sin^2\alpha + cos^2\alpha} \quad (3)$$

$$k_{90} = 1.35 + 0.015d \quad (4)$$

where the characteristic wood density is ρ_k, the characteristic tensile strength of the steel material is $f_{u,k}$ and the angel between the fibre direction and the dowel force direction is α. The two limit-thicknesses t_{I-II}, and t_{II-III} shown in Figure 1 are given by

$$\begin{bmatrix} t_{I-II} \\ t_{II-III} \end{bmatrix} = \begin{bmatrix} \sqrt{e^2 + \frac{2M_{y,Rk}}{f_{h,\alpha,k} d}} - e \\ \sqrt{\frac{4M_{y,Rk}}{f_{h,\alpha,k} d}} + \sqrt{e^2 + \frac{4M_{y,Rk}}{f_{h,\alpha,k} d}} - e \end{bmatrix} \quad (5)$$

Failure mode *I* is a pure compressional failure of the wood material caused by a constant plastic embedment deformation over the cross-sectional thickness. This failure mode arises for small wood thicknesses ($t < t_{I-II}$), where the maximum moment in the dowel does not reach the yield moment of the dowel. Failure mode *II* is a mixed steel/wood failure caused by varying embedment deformation over the wood thickness. It occurs for larger wood thicknesses ($t_{I-II} \leq t < t_{II-III}$), when a yield hinge in the shear plane has developed together with plastic compressional failure of the wood material caused by combined translational and rotational embedment deformations. Failure mode *III* is also a mixed steel/wood failure caused by varying embedment deformation over a part of the wood thickness. This occurs for large thickness

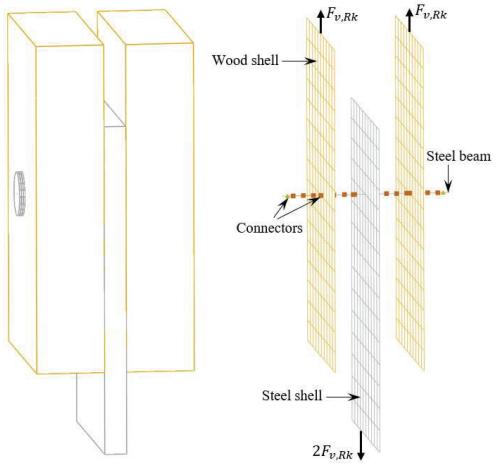

Figure 2: *Illustration of the beam and shell elements used to simulate the single dowel double shear joint.*

values ($t_{II-III} \leq t$), where the plastic clamping moment of the wood member is equal or larger than the yield moment of the dowel. Note that the expressions in Eq. (1) have no criterion concerning maximum embedment deformation related to the risk of crack initiation. The challenge here is to develop an effective FE-model (in a 3D-space) that can simulate both the different failure modes and realistic (slip-driven) elastic and plastic embedment deformations. To achieve model efficiency, the wood members and steel plate were modelled with shell elements and the fastener with beam elements; see Figure 2. Special nonlinear connector elements were also used to connect the different joint members. Both translational and rotational springs were used to model the constantly respective linearly varying elastic and plastic embedment deformations over the wood thickness. This allows us to simulate both the generation of yield hinges in the steel dowel (beam elements) and plastic embedding failure in the wood material (connector elements). The static dowel models for the three different failure modes are shown in Figure 3. The two yellow springs (translational and rotational) in Figure 3 show the two wood-to-dowel connectors used to simulate the embedment deformation of the wood. The yellow strokes parallel to the dowels represent the mechanical contacts

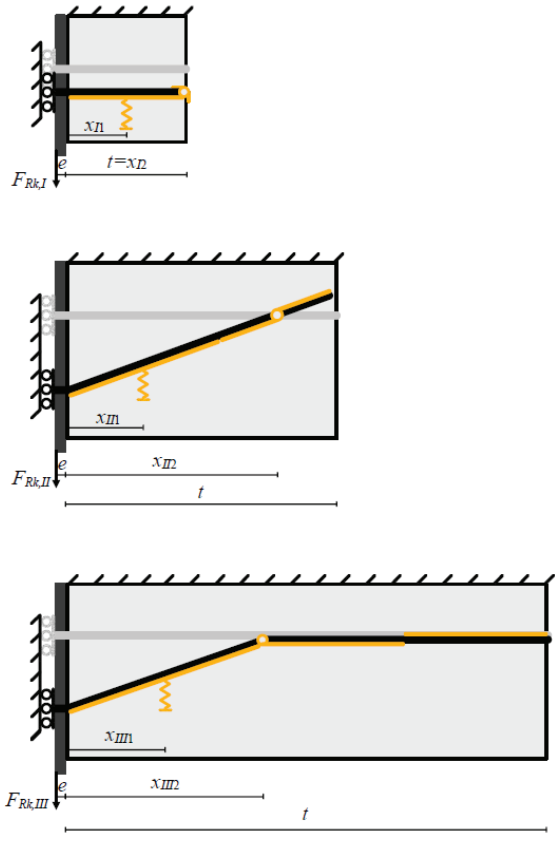

Figure 3: *Static beam-connector models used for the dowels at failure (i.e., failure modes I, II and III).*

between the wood and the dowels. Therefore, the three translational springs represent springs distributed along the lengths ($2x_{I1}$, $2x_{II1}$ and $2x_{III1}$). The translational and rotational spring stiffnesses ($k_{Iu}, k_{IIu}, k_{IIIu}$) and ($k_{I\theta}$, $k_{II\theta}$, $k_{III\theta}$) as well as the yield force ($P_{Iy,w}, P_{IIy,w}$, $P_{IIIy,w}$) and clamping moments ($M_{Iy,w}$, $M_{IIy,w}$, $M_{IIIy,w}$) for the different failure modes are calculated as

$$\begin{bmatrix} k_{Iu} \\ k_{I\theta} \\ k_{IIu} \\ k_{II\theta} \\ k_{IIIu} \\ k_{III\theta} \end{bmatrix} = \begin{bmatrix} \frac{E_{\alpha,k} x_{I1} d}{l_{\alpha,t,I}} \\ 0 \\ \frac{2E_{\alpha,k} x_{II1} d}{l_{\alpha,t,II}} \\ \frac{2E_{\alpha,k} x_{II1} d}{l_{\alpha,t,II}} (t - x_{II2})^2 \\ \frac{2E_{\alpha,k} x_{III1} d}{l_{\alpha,t,III}} \\ \frac{2E_{\alpha,k} x_{III1} d}{l_{\alpha,t,III}} \left(\frac{3(t - x_{III2})}{4}\right)^2 \end{bmatrix} \tag{6}$$

$$\begin{bmatrix} P_{Iy,w} \\ M_{Iy,w} \\ P_{IIy,w} \\ M_{IIy,w} \\ P_{IIIy,w} \\ M_{IIIy,w} \end{bmatrix} = \begin{bmatrix} 2f_{h,\alpha,k} d x_{I1} \\ 0 \\ 2f_{h,\alpha,k} d x_{II1} \\ f_{h,\alpha,k} d (t - x_{II2})^2 \\ 2f_{h,\alpha,k} d x_{III1} \\ f_{h,\alpha,k} d \left(\frac{(t - x_{III2})}{2}\right)^2 \end{bmatrix} \tag{7}$$

where $E_{\alpha,k}$ is the effective modulus of elasticity in the dowel force direction and ($l_{\alpha,t,I}$, $l_{\alpha,t,II}$, $l_{\alpha,t,III}$) are the effective lengths for the embedment deformations in the dowel force direction. Finally, the lengths shown in Figure 3 are defined as

$$\begin{bmatrix} x_{I1} \\ x_{I2} \\ x_{II1} \\ x_{II2} \\ x_{III1} \\ x_{III2} \end{bmatrix} = \begin{bmatrix} \frac{1}{2}t \\ t \\ \frac{\sqrt{(t+2e)^2 + t^2 + \frac{4M_{yRk}}{f_{h,\alpha,k} d}} - t - 2e}{2} \\ \frac{1}{2}\sqrt{(t+2e)^2 + t^2 + \frac{4M_{yRk}}{f_{h,\alpha,k} d}} - e \\ \frac{1}{2}\left(\sqrt{e^2 + \frac{4M_{yRk}}{f_{h,\alpha,k} d}} - e\right) \\ \sqrt{e^2 + \frac{4M_{yRk}}{f_{h,\alpha,k} d}} - e \end{bmatrix} \tag{8}$$

2.2 A BEAM MODEL USING TWO CONNECTORS FOR EACH DOWEL GROUP

Deflection of mechanically jointed timber beams is difficult to calculate manually, especially if the beams are unsymmetric and the connections are exposed to both

https://doi.org/10.52202/069179-0172

shear and moment action. To simulate bending of a jointed glulam with a slotted-in steel plate connection, a simple beam model in a 3D-space was created. To reduce the model size, the mechanical connections between the steel plate and wooden members were modelled with two nonlinear connector elements for each dowel group. The model geometry and locations of beams, connectors and coupling constraints for cross sections are shown in Figure 4.

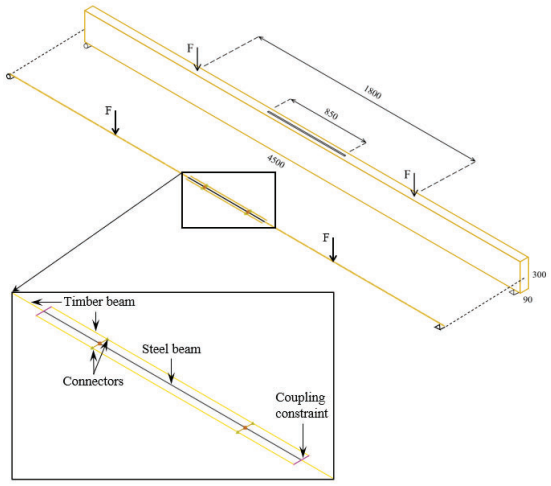

Figure 4: *A beam model of the jointed glulam which also visualizes a 3D-sketch of the beam and a close-up picture showing the most important elements in the connection part.*

Figure 4 shows how beam elements are used for the wooden members and the steel plate. To ensure that each half of the glulam will work as a single member, the two wood beams beside the steel plate are coupled (with a kinematic constraint) to the end-beams. For each shear plane between the steel plate and the wood members the joint behaviour of each dowel group was modelled with only one nonlinear connector. The connectors are placed in the centre of gravity of the dowel group and consist of three uncoupled springs to model the relative in-plane slip deformations caused by normal, shear and moment action in the joint. The stiffness values of the springs are calculated according to Eq. (9), where $E_{m,0}$, $E_{m,90}$ and $E_{m,\alpha i}$ are the mean modulus of elasticity for varying dowel force directions, l_0, l_{90} and $l_{\alpha i}$ are effective lengths for the local embedding deformation, r_i is the radii from the centre of gravity of the dowel group to the different dowels and n is number of dowels in each dowel group. To model the (ideal plastic) dowel group failure at the ultimate load, a failure moment for the rotational spring

$$\begin{bmatrix} k_N \\ k_V \\ k_M \end{bmatrix} = \begin{bmatrix} n\dfrac{E_{m,0}td}{l_0} \\ n\dfrac{E_{m,90}td}{l_{90}} \\ td\displaystyle\sum_{i=1}^{n}\dfrac{E_{m,\alpha i}}{l_{\alpha i}}r_i^2 \end{bmatrix} \quad (9)$$

was defined based on the experimental results in [10], briefly described in Section 3. This model is parametrized, i.e., it can easily be used to study how different joint configurations will influence the bending deformations of the mechanically jointed glulam beams.

2.3 A BEAM-SHELL MODEL USING A FEW CONNECTORS FOR EACH DOWEL

To simulate global bending deformations, failure modes and progressive development of the elasto-plastic force distributions in all dowels, a combined beam-shell model was created, see Figure 5.

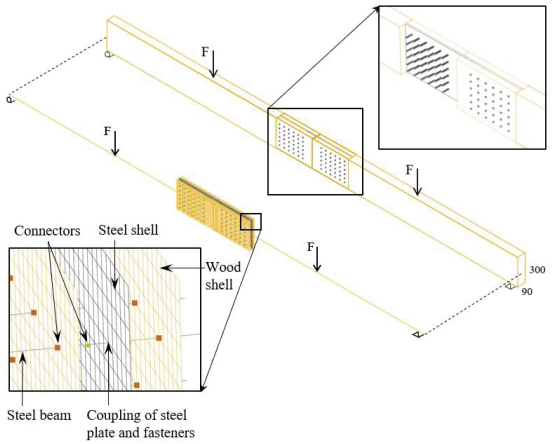

Figure 5: *A beam-shell model of the jointed glulam which also visualises a 3D-sketch of the beam and two close-up pictures showing a dowel group and the most important elements in the connection part.*

For the connection part, the wooden side members and the steel plate are modelled with shell elements, while all the steel dowels are modelled with small beam elements. The two wood shells are coupled (with kinematic constraints) to the beam elements used to model the remaining part of the glulam. The beams for the steel dowels are used as fastener elements between the steel plate and the wooden side members. Interaction between these beams and the steel and wood shells are modelled with nonlinear connector elements. Both elastic and plastic properties of the connectors are defined as for the single joint model.

3 EXPERIMENTAL STUDY

To verify the numerical model, several full-sized glulam beams with a mid-span slotted-in steel plate connection were tested in four-point bending until failure. The tests were performed at an ambient climate, with a temperature range of 20-25 °C. In total, six beams with cross-sectional dimensions of 90x300 mm were tested. Each specimen was constructed of eight stress graded wood lamellae from Norway spruce. The beams were divided into two groups, A with 10 mm dowels and B with 20 mm dowels. Beam assembly resulted in three density classes (DL, DM and DH) for each group. The average moduli of elasticity were 14.3, 15.1 and 15.7 GPa for group A and 14.2, 15.1

https://doi.org/10.52202/069179-0172

and 16.1 GPa for group B. The beams were cut into two equal parts and then re-jointed with a mechanical slotted-in steel plate connection, as shown in Figure 6.

Figure 6: *Glulam beams jointed with mechanical slotted-in steel plate connections.*

The dowel length was 100 mm, and the total number of dowels were 72 for group A and 24 for group B; see the detailed drawings of the connections in Figure 7. The dowel groups are quite different, but the rotational stiffness of group A is only 22% larger than of group B. Throughout the entire experiment, the force-displacement relationship was measured for the maximum mid-span deflection. Figure 8 shows this relationship for all the tested beams. The test results show almost similar linear relationships all the way up to the first crack initiation, when the force significantly drops followed by a jagged curve that on average is quite horizontal under a certain increase of the deflection.

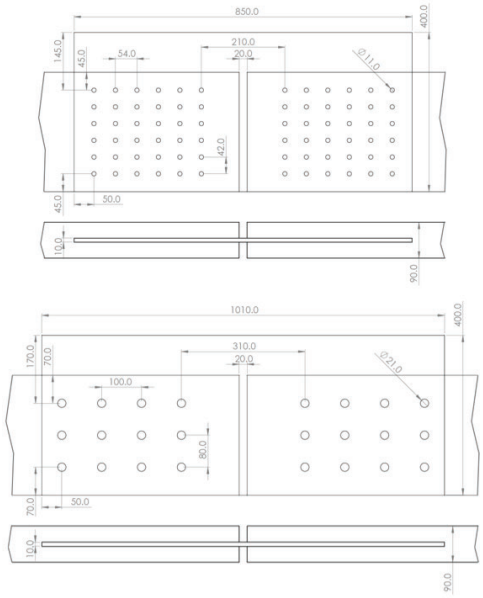

Figure 7: *Connection drawings showing the most important geometrical measures for dowel groups A and B.*

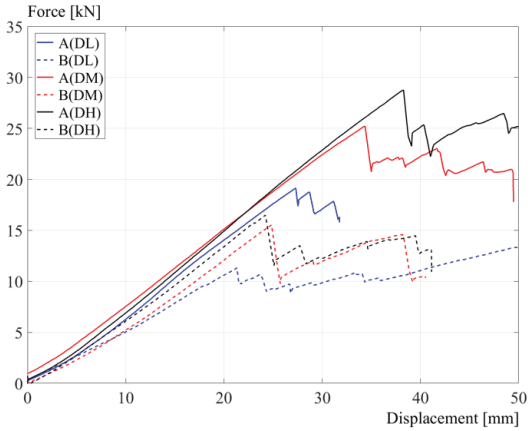

Figure 8: *Experimentally obtained force-displacement relationship for all the beams studied.*

Most of the connection failures show cracks that propagated between the bottom dowels and occasionally between the top dowels. Figure 9 shows two pictures of typical failure appearances for dowel groups A and B.

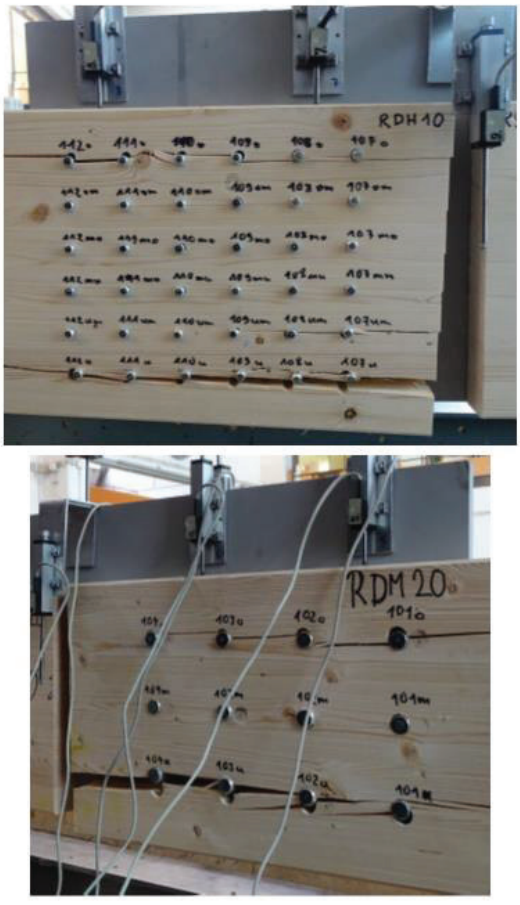

Figure 9: *Typical failure appearances of the slotted-in steel plate connections for groups A and B.*

https://doi.org/10.52202/069179-0172

4 RESULTS AND DISCUSSION

Simulation results are here presented and discussed to show certain outputs from the models.

4.1 SINGLE DOWEL MODEL

The single dowel model was used to simulate deformations and dowel forces in slotted-in steel plate joints of different thicknesses. Figure 10 shows simulated failure modes of three different single dowel joints together with simulated and manually calculated curves that show how the shear load carrying capacity of the joint varies with increasing wood thickness.

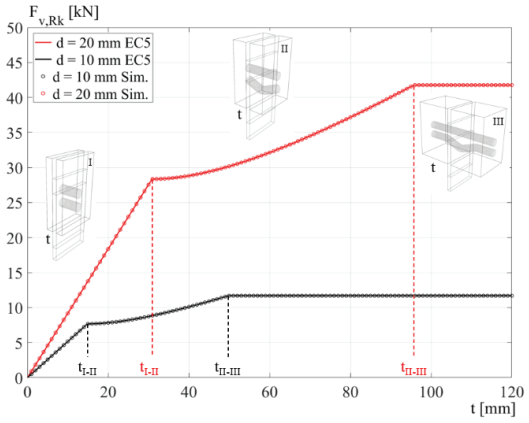

Figure 10: *Comparison of simulated and manually calculated curves showing variation in shear load carrying capacity with increasing wood thickness together with simulated failure modes of the joints.*

Figure 10 shows exact match between simulated and manually calculated load carrying capacity curves as the expected failure modes develop. However, to obtain good results, properly defining the location of the connectors and how to calculate the clamping moment of the dowels are essential. This also allowed us to consider the eccentricity of the fastener forces in the shear joint.

4.2 A BEAM MODEL USING TWO CONNECTORS FOR EACH DOWEL GROUP

This simple model was used to simulate the global bending deformations and (ideal plastic) load carrying capacity of the two tested beam types A and B. The beams had the same geometry, though they had different dowel groups; see Figure 7. The material data used in the model was mainly obtained from the test results. To illustrate some of the model outputs, Figure 11 shows typical bending deformation of beam A together with a close-up figure of the connection part. For a load of $F = 15$ kN, the maximum deflection became $u_{max} = 20.8$ mm. A similar deflection value for beam B is approximately 4% larger than for beam A. The connection of beam A thus reduces the bending stiffness by 19.2% compared with a continuous beam of the same dimensions. This could also be seen as 16.7% reduction of the cross-sectional height in the connection area.

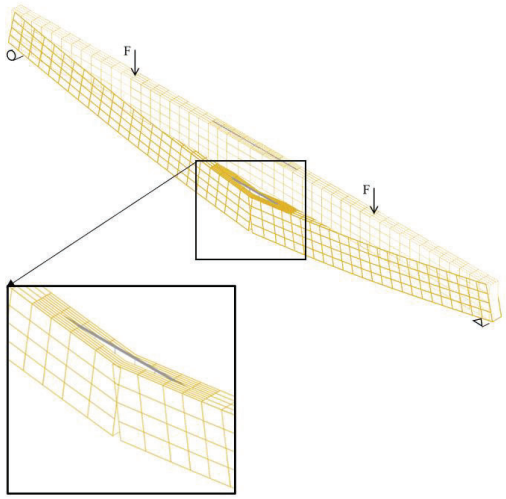

Figure 11: *Magnified bending deformation of the glulam beam A for F = 25 kN.*

The experimental results in Section 3 show a linear relationship between the external load and the deflection all the way up to failure. A typical failure occurs when cracking propagates between the bottom dowels. When cracking starts, the force drops slightly and then maintains a constant or slightly decreasing value under a certain increase of deflection. These test results were used to calibrate the model regarding stiffness and yield moment of the rotational spring. Figure 12 shows the simulated results with the experimentally obtained curves for the three glulam beams of type A. To illustrate the flexibility of the model, Figure 13 shows the bending deformation of the unsymmetric glulam beam jointed with a similar connection that is subjected to both shear and moment loading. The close-up figure in Figure 13 shows clearly the unsymmetric deformation in the connection due to the varying moment and shear forces over the length of the connection.

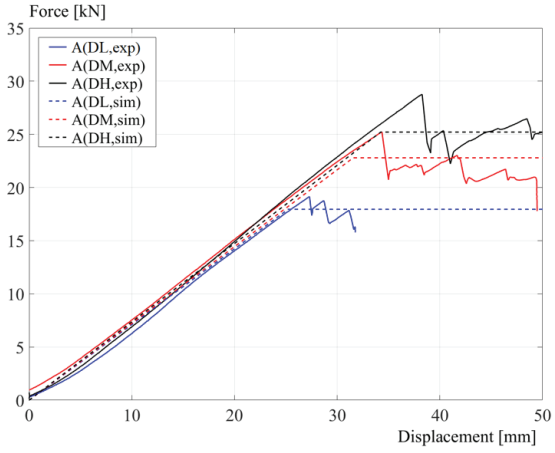

Figure 12: *Simulated and experimentally obtained force-displacement curves for the three beams of type A.*

https://doi.org/10.52202/069179-0172

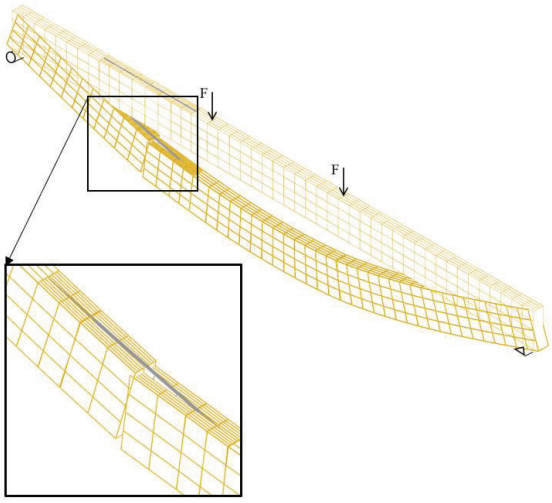

Figure 13: *Magnified bending deformation of an unsymmetric glulam beam with a mechanical connection exposed to both shear and moment action.*

4.3 BEAM-SHELL MODEL WITH A FEW CONNECTORS FOR EACH FASTENER

This model was used to simulate the experimental beams A and B to study how bending deformation and fastener force distribution develop in multiple fastener connections during progressive plasticization of the dowels.

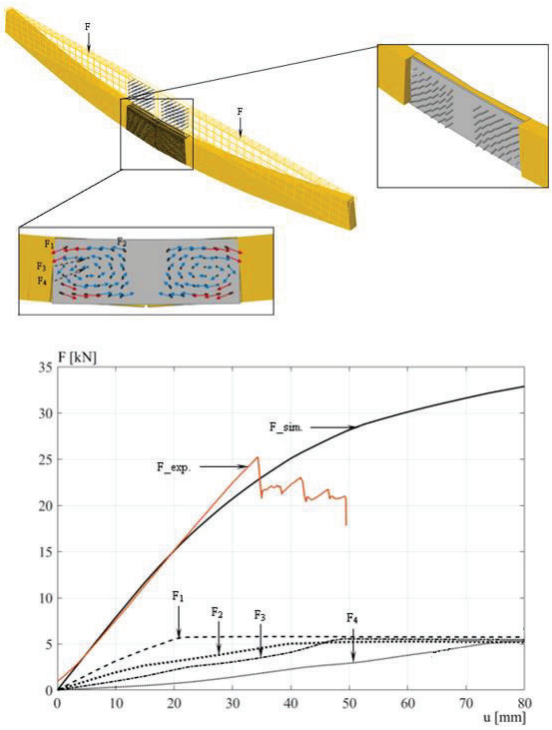

Figure 14: *Simulated bending deformation and fastener force vectors at F = 22 kN as well as simulated and experimentally obtained force-deflection relationships.*

Figures 14*(a)* and 15*(a)* show simulated bending deformations and fastener force distributions when the beams are loaded with F = 22 kN. The bending of the beams is quite similar, though beam B is slightly more curved. The fastener force distribution in beam A shows several plasticized dowels (red arrows), whereas beam B shows none (only blue arrows). The largest forces arose at the corners of the dowel groups, and their directions deviated somewhat from those used in manual calculations. Figures 14*(b)* and 15*(b)* show that the numerical force-deflection curve for beam A fit well with the test results up to a certain force value. However, the conformity was not as good for beam B. To better illustrate the dowel plasticization, the subfigure 14(*b)* also shows elasto-plastic shear force development of some selected fasteners in the dowel groups. The results show clearly how these dowels progressively plasticize during increased loading. The numerical modelling of these beams is based on stiffness data from the experimental study.

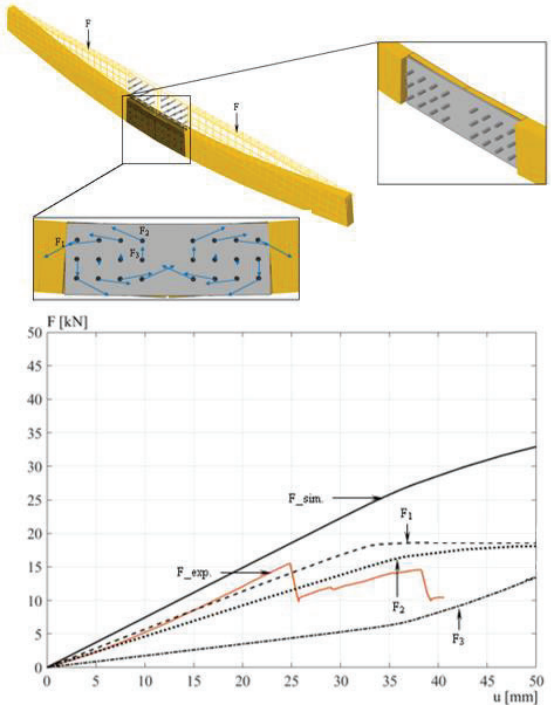

Figure 15: *Simulated bending deformation and fastener force vectors at F = 22 kN as well as simulated and experimentally obtained force-deflection relationships.*

5 CONCLUSION

This work focuses on simple and effective modelling of mechanically jointed glulam beams with slotted-in steel plate connections. The simulation models use beam, shell, and connector elements together with analytical expressions and failure modes from EC5. The single dowel model can simulate both elastic and plastic embedment behaviour of the joints in the form of

https://doi.org/10.52202/069179-0172

deformations and different failure modes. As well, the model was directly implemented when simulating multiple fastener connections where progressive plasticization of the dowel groups was studied during increased loading. Based on the experimental verification, it can be concluded that this model is useful to simulate bending behaviour and failure modes of mechanically jointed timber beams in a constant climate condition. Most numerical results agreed well with the experimental findings up to a certain level of deformation. All experimental results confirmed that these types of connections have low plastic utilization of the dowels, and instead failed in relativity brittle cracking of the wood material. An interesting fact is that beams A have slightly higher bending stiffness but almost double the load carrying capacity of beams B. This indicates that the dowels diameter has a significant impact on the load carrying capacity of jointed glulam beams exposed to dominating moment loading. Based on the experimental observation, a simple beam model was created and used to simulate both global bending deformations and (ideal plastic) load carrying capacity of the two tested glulam beams. It also turned out that the elastic load carrying capacity (with only plasticization in the corner dowels) according to manual EC5 calculations was ca 17% lower than the experimental failure value for beam A(DL) and ca 60% higher for beam B(DL).

A major advantage of the models presented are their short computational time compared to 3D models. It is concluded that these models are useful to simulate bending deformations, fastener forces and failure modes of mechanically jointed timber beams. As well, they have good potential for further development regarding large deformations to simulate rope effect in bolts and screws and moisture related dowel forces.

REFERENCES

[1] K. W. Johansen, “Theory of timber connections,” *Int Assoc Bridge Struct Eng*, vol. 9, pp. 249–262, 1949, doi: 10.5169/seals-9703.

[2] B. H. Xu, M. Taazount, A. Bouchaïr, and P. Racher, “Numerical 3D finite element modelling and experimental tests for dowel-type timber joints,” *Constr Build Mater*, vol. 23, no. 9, pp. 3043–3052, Sep. 2009, doi: 10.1016/j.conbuildmat.2009.04.006.

[3] B. H. Xu, A. Bouchaïr, M. Taazount, and E. J. Vega, “Numerical and experimental analyses of multiple-dowel steel-to-timber joints in tension perpendicular to grain,” *Eng Struct*, vol. 31, no. 10, pp. 2357–2367, Oct. 2009, doi: 10.1016/j.engstruct.2009.05.013.

[4] M. Basterrechea-Arévalo, J. M. Cabrero, B. Iraola, and R. Goñi, “Modelling of moment transmitting beam-to-column timber connections accounting for frictional transmission,” *Eng Struct*, vol. 247, Nov. 2021, doi: 10.1016/j.engstruct.2021.113122.

[5] S. Ormarsson, O. Dahlblom, M. J. Nygaard, “Finite Element Simulation of Mechanical and Moisture-Related Stresses in Laterally Loaded Multi-Dowel Timber Connections,” *In* WCTE 2010 World Conference on Timber Engineering, June 20-24, 2010, Riva del Garda, Trentino, Italy.

[6] A. Bouchaïr, P. Racher, and J. F. Bocquet, “Analysis of dowelled timber to timber moment-resisting joints,” *Materials and Structures/Materiaux et Constructions*, vol. 40, no. 10, pp. 1127–1141, Dec. 2007, doi: 10.1617/s11527-006-9210-0.

[7] M. Schweigler, T. K. Bader, and G. Hochreiner, “Engineering modeling of semi-rigid joints with dowel-type fasteners for nonlinear analysis of timber structures,” *Eng Struct*, vol. 171, pp. 123–139, Sep. 2018, doi: 10.1016/j.engstruct.2018.05.063.

[8] R. and B. J.-F. and S. M. and B. T. K. Lemaitre, “Beam-on-Foundation Modelling as an Alternative Design Method for Timber Joints with Dowel-Type Fasteners: Part 2: Modelling Techniques for Multiple Fastener Connections,” in *6th meeting of INTER (International Network on Timber Engineering Research*, 2019.

[9] M. Mahjoub, “FE modeling of glulam beams with mechanical slotted-in steel plate connections,” Master thesis, Linnaeus University, Växjö, 2021.

[10] K. Simon, S. Aicher, S. Ormarsson and J. Vessby, “Report 1: Materials, specimen manufacture and ramp load reference tests,” MPA University of Stuttgart, 2021.